Parameters Influencing Charge Recombination Kinetics in Dye-Sensitized Nanocrystalline Titanium Dioxide Films

Saif A. Haque,[†] Yasuhiro Tachibana,[†] Richard L. Willis,[†] Jacques E. Moser,[‡] Michael Grätzel,[‡] David R. Klug,[†] and James R. Durrant*,[†]

Centre for Photomolecular Sciences, Departments of Chemistry and Biochemistry, Imperial College of Science, Technology and Medicine, London SW7 2AY, U.K., and Institut de Chimie Physique, École Polytechnique Fédérale de Lausanne, CH-1015 Lausanne, Switzerland

Received: March 30, 1999

Optical excitation of Ru^{II}(2,2′-bipyridyl-4,4′dicarboxylate)$_2$(NCS)$_2$-sensitized nanocrystalline TiO_2 films results in injection of an electron into the semiconductor. This paper addresses the kinetics of charge recombination which follows this charge separation reaction. These charge recombination kinetics were found to be strongly dependent upon excitation intensity, electrolyte composition, and the application of an electrical bias to the TiO_2 film. For excitation intensities resulting in less than one excited dye molecule/TiO_2 particle, the recombination kinetics were independent of excitation intensity. Increasing the excitation intensity above this level resulted in a rapid acceleration in the charge recombination kinetics. Similarly, for positive electrical potentials applied to the TiO_2 electrode, the recombination kinetics were independent of applied potential. If the applied potential was more negative than a threshold potential V_{kin}, a rapid acceleration of the charge recombination kinetics was again observed, for example from ∼1 ms at +0.1 V vs Ag/AgCl to ∼3 ps at −0.8 V (∼10^8 fold increase in the rate). Moreover, at a constant applied potential the charge recombination kinetics were found to be strongly dependent upon electrolyte composition (up to 10^6-fold change in rate). This strong dependence upon the electrolyte composition was found to be associated with shifts in the threshold potential V_{kin}. Spectroelectrochemical measurements were used to monitor the shift in the trap/conduction band density of states induced by the electrolyte composition. A direct correlation was observed between the threshold voltage V_{kin} observed from kinetic measurements, and the threshold voltage for electron occupation of conduction band/trap states of the TiO_2 observed from spectroelectrochemical measurements. This direct correlation was observed for a wide range of electrolyte compositions including protic and aprotic solvents and the addition of Li^+ ions and 4-*tert*-butylpyridine. We conclude that the charge recombination kinetics in such dye-sensitized films are strongly dependent upon the electron occupation in trap/conduction band states of the TiO_2 film. This occupation may be modulated by variations in light intensity, applied electrical potential, and electrolyte composition. These results are discussed with relevance to the function of dye-sensitized photoelectrochemical devices.

Introduction

Wide band gap semiconductors can be sensitized to visible light by the adsorption of molecular dyes to their surface. Interest in these processes has recently been increased by developments in dye-sensitized photovoltaic devices.[1−3] The function of such devices is based upon the injection of an electron from a photoexcited state of the sensitizer dye into the conduction band of the semiconductor. Attention has focused upon nanocrystalline semiconductor films, due in particular to the high surface areas of such films available for dye adsorption. Nanocrystalline TiO_2 films, sensitized by the dye Ru^{II}(2,2′-bipyridyl-4,4′-dicarboxylate)$_2$(NCS)$_2$ (Ru(dcbpy)$_2$(NCS)$_2$), have yielded the most efficient dye-sensitized photovoltaic devices reported to date.[2] Most such devices employ a liquid electrolyte comprising, typically, an iodide/triiodide redox active couple in acetonitrile. The function of this redox couple is to rereduce the dye cation, following electron injection, and transport the resulting positive charge to the counter electrode.

The kinetics of electron transfer at the semiconductor/dye/electrolyte interface are critical to the efficiency of the device. The rate of electron injection must be greater than the decay of the dye excited state to ground. In addition, the rate of rereduction of the dye cation by I^- must be greater than recombination of this dye cation with electrons injected into the semiconductor. There is now a growing consensus that the electron injection process, in dye-sensitized nanocrystallineTiO_2 films, can proceed on subpicosecond time scales for a range of different sensitizer dyes.[4−11] We recently found that these injection kinetics are moreover rather insensitive to variations in experimental conditions (e.g., electrolyte composition and application of electrical bias[6,11]). In contrast, the corresponding charge recombination reaction between injected electrons and dye cations has been reported to exhibit time constants ranging from picoseconds to milliseconds.[12−21] Previous studies have considered a range of different sensitizer dyes, semiconductor materials, and electrolyte compositions. However, agreement over the parameters underlying the large variation in experimental time constants has been limited to date.[12] This is particularly relevant to the development of dye-sensitized photovoltaic devices because there is increasing evidence that

* Corresponding author (Fax: (44) 171 225 0960; E-mail: J.Durrant@ic.ac.uk).
[†] Imperial College of Science, Technology, and Medicine.
[‡] École Polytechnique Fédérale de Lausanne.

10.1021/jp991085x CCC: $19.00
Published on Web 12/28/1999

this charge recombination process may play an important role in limiting device efficiency.[22−24]

We recently reported that the application of an external electrical bias to a dye-sensitized TiO_2 electrode in the presence of a redox inactive electrolyte can result in a rapid acceleration of the rate of charge recombination.[23] In particular, a change in the bias voltage by 500 mV resulted in a reduction in the median time constant of charge recombination from approximately 1 ms to less than 100 ns. The kinetics were also found to exhibit highly nonexponential behavior. When compared with the kinetics observed in the presence of an iodide redox couple, where a 100 ns rereduction of the dye cation by the iodide was observed, it was apparent that the charge recombination process may result in a significant loss of photocurrent depending upon the voltage applied to the semiconductor and may limit the open circuit voltage of the device. Although a more quantitative analysis clearly requires careful consideration of other aspects of device function,[25] these observations clearly demonstrated the potential importance of charge recombination between injected electrons and dye cations in limiting device function. This charge recombination process had been largely neglected in previous numerical models that were primarily based upon frequency domain analyses of device function.[49−52]

Dye-sensitized photovoltaic devices generally employ nanocrystalline metal oxide films, because the high surface area of these films allows efficient light absorption for a monolayer of adsorbed sensitizer dyes. Such nanocrystalline TiO_2 films have been widely reported to exhibit a high density of sub-bandgap or "trap" states attributed, at least in part, to surface states.[1,26−30] We have suggested that both the nonexponential recombination kinetics and the strong dependence upon applied bias may be associated with these trap states.[23] The acceleration in the charge recombination kinetics at negative applied potentials was tentatively attributed to an increase in the electron occupancy of these trap states as the semiconductor Fermi level was raised.[23]

Spectroelectrochemical techniques have been used to investigate the dependence of the potential of the conduction band edge upon the electrolyte composition. This edge has been shown to exhibit a Nernstein shift as a function of electrolyte proton activity, shifting by 59 meV per pH of the electrolyte.[31] In addition to protons, other small cations such as Li^+ and Mg^{2+} have also been found to have a strong influence upon the conduction band energy of these films. For example, the addition of 0.1 M Li^+ to an aprotic solvent such as acetonitrile was found to result in a shift of the conduction band edge of the film by more than 1 V.[32] This observation has particular technological relevance because Li^+ cations are typically added to the electrolyte of dye-sensitized photovoltaic devices in order to increase the efficiency. The cause of this increase in efficiency, and its correlation with the influence of the Li^+ on the conduction band energetics is unclear.

In this paper we address further the parameters controlling the kinetics of charge recombination in dye-sensitized nanocrystalline semiconductor films. In particular, we investigate the correlation between the occupancy of conduction band/trap states of the TiO_2 and the kinetics of charge recombination. We conclude that these kinetics are largely controlled by the electronic occupancy of conduction band/trap states within the TiO_2.

Materials and Methods

Sample Preparation. Nanocrystalline titanium dioxide films were prepared on fluorine-doped SnO_2 conducting glass (17 Ω). Nanocrystalline TiO_2 films were prepared following previously published methods (Nazeeruddin et al.[2] method A). The resulting films were 8 μm thick and comprised 15 nm diameter anatase particles (approximately 3×10^{14} nanoparticles/cm^2). Ru(dcbpy)$_2$(NCS)$_2$ was synthesized following Nazeerudin et al.[2] The adsorption of the dye on nanocrystalline TiO_2 films was achieved by immersion in 2×10^{-5} M ethanolic solutions of these dyes at room temperature for 8 h. The resulting films had optical densities of 0.3 at 538 nm (sample absorption maximum) which corresponds to dye coverages of approximately one-fifth of a monolayer. After the sensitization procedure the films were covered with a 1:1 ethylene carbonate/propylene carbonate (EC/PC) solvent mixture and a thin glass cover slide. All the samples were stored under dry conditions and in the dark. All experiments were conducted at room temperature (295 K).

Potential Control. For experiments under bias control, the dye-sensitized titanium dioxide film formed the working electrode (∼1 cm^2 macroscopic area) in a three-electrode photoelectrochemical cell employing a platinum wire counter electrode and an Ag/AgCl reference electrode. Potential control was provided by a home-built potentiostat as described previously.[23] Electrolyte solutions were prepared from acetonitrile (Fluka GLC grade) or ethanol (Analar 99.7%) using 0.1 M tetrabutylammonium perchlorate, TBAP (Sigma grade) and tetrabutylammonium triflate, TBAT (99% grade Aldrich), respectively. The composition was further adjusted by using $LiClO_4$ (Sigma grade) and 4-*tert*-butylpyridine (Aldrich) as appropriate. The acetonitrile was distilled over CaH_2 prior to use to minimize water content. The current drawn by the cell was monitored during all experiments. This current was 1−10 μA, depending upon applied bias, during all experiments and was unchanged by any of the measurement or excitation light beams used during the spectroscopic experiments.

Spectroscopy. Spectroelectrochemical measurements were conducted by incorporating the photoelectrochemical cell into the sample compartment of a spectrophotometer (Perkin-Elmer 554 or Shimadzu UV1601). Nanosecond to millisecond transient absorption spectroscopy was performed as described previously.[23] The excitation wavelength was set at 560 nm, except for studies at high excitation intensities (Figure 1), where the excitation wavelength was 532 nm (pulse durations of ∼600 ps and 10 ns, respectively; repetition rate of 2 Hz). At these excitation wavelengths sample optical density was dominated by sensitizer dye absorption. The probe wavelength was set to monitor the transient signal at 820 nm, which primarily results from Ru(dcbpy)$_2$(NCS)$_2$ cation absorption, as previously assigned.[4]

Details of the ultrafast transient absorption experiments are reported elsewhere.[11] Experiments employed 525 nm excitation pulses (duration 150 fs) at 1 kHz repetition rate, and white light probe pulses with multichannel data collection. The instrument response was 250 fs.

All of the transient data were collected employing low-intensity excitation pulses unless otherwise stated (0.1−0.3 mJ/cm^2 at 560 nm and 0.12 mJ/cm^2 at 532 nm for the nanosecond−millisecond measurements, and 0.2 mJ/cm^2 at 525 nm for the ultrafast measurements). The number of injected electrons per nanoparticle was estimated both by determination of the number of absorbed photons per unit area and by consideration of the magnitude of the dye ground-state absorption bleach resulting from cation formation (employing a difference extinction coefficient at 540 nm of 12 000 Mcm^{-1} obtained from previously published data[4]). These two methods yielded indistinguishable results within experimental uncertainties (±50%). All

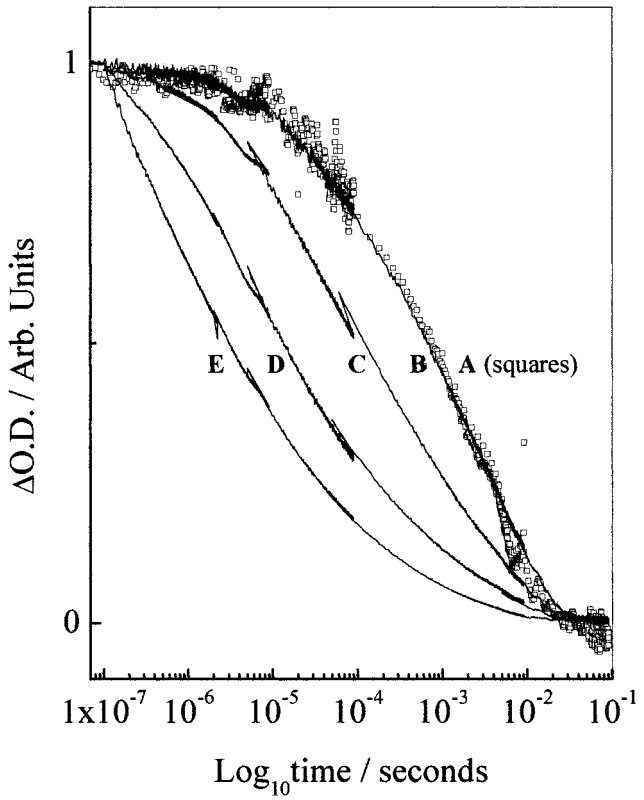

Figure 1. Transient absorption data following the decay of the cation state of $Ru(dcbpy)_2(NCS)_2$ absorbed on a nanocrystalline TiO_2 film. Cation decay is attributed to charge recombination with electrons in trap/conduction band states of the TiO_2. Data were collected at a probe wavelength of 820 nm employing 525 nm excitation pulses. Data are shown for different excitation intensities. (A) 0.04, (B) 0.12, (C) 0.6, (D) 3.5, and (E) 6 $mJcm^{-2}$. All data shown here were collected employing an ethylene carbonate/propylene carbonate electrolyte (1:1 ratio).

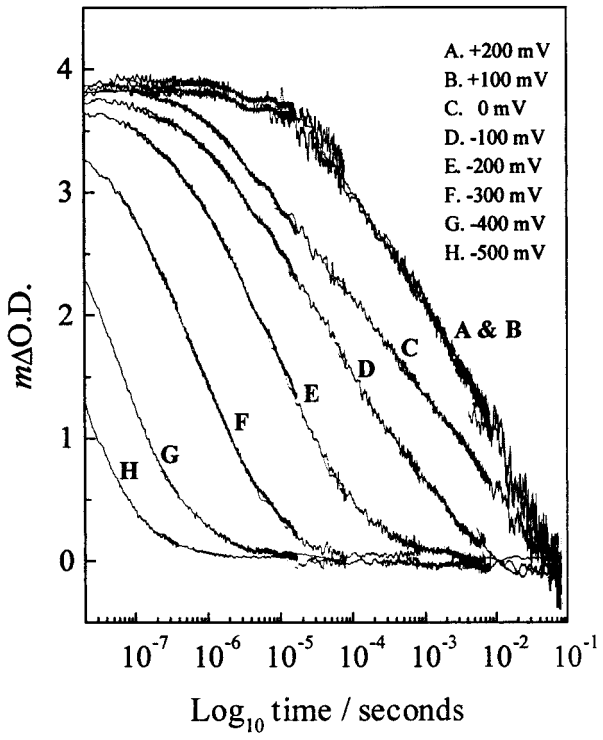

Figure 2. Transient absorption data following the decay of the cation state of $Ru(dcbpy)_2(NCS)_2$ adsorbed on a TiO_2 nanocrystalline electrode as a function of applied potential. Cation decay is attributed to charge recombination with electrons in trap/conduction band states of the TiO_2. Data were collected at a probe wavelength of 820 nm in a three-electrode photoelectrochemical cell at room temperature, employing 560 nm excitation pulses and an ethanol/0.1 M TBAT electrolyte (electrolyte A). The electrolyte was maintained at a constant potential by an Ag/AgCl reference electrode. Data shown range from +200 to −500 mV vs Ag/AgCl.

transient experiments employed excitation densities corresponding to $\leq 1 \pm 0.5$ excited dye molecule/nanoparticle unless otherwise stated. These conditions correspond to excitation of ~3% of the dye molecules per excitation pulse. The effect of applied bias potential upon the transient kinetics of charge recombination was fully reversible. Indistinguishable data were observed at 0 V at the beginning and the end of each experimental run.

Results

Following pulsed excitation of nanocrystalline TiO_2 films sensitized by $Ru(dcbpy)_2(NCS)_2$, a broad absorption increase is observed to peak at ~800 nm corresponding to formation of the dye cation state.[4,33−35] In the absence of a redox active electrolyte, this cation state is rereduced by charge recombination with electrons occupying conduction band/trap states of the TiO_2.[23] Monitoring the decay kinetics of this photoinduced absorption is therefore a probe of this charge recombination.

The kinetics of this charge recombination are strongly dependent upon the experimental conditions employed. We consider first the influence of excitation intensity. Figure 1 shows absorption transients at 820 nm as a function of excitation intensity employing 532 nm excitation pulses. The transients are plotted on a logarithmic time scale and exhibit multiexponential kinetics. The recombination kinetics are independent of excitation intensities for intensities below 0.12 mJ/cm^2 (consistent with our estimate of $\sim 1 \pm 0.5$ photoinduced dye cations per TiO_2 particle at this excitation intensity; see Materials and Methods). As the excitation intensity is increased beyond this level, the recombination kinetics speed up by a factor of at least 10^3 times resulting from an increase in excitation power from 120 $\mu J/cm^2$ to 6 mJ/cm^2. As discussed below, this nonlinear behavior arises from the injection of more than one electron per particle. A quantitative analysis of these kinetics is, however, precluded by our observation that even for moderate excitation intensities (≥ 0.6 mJ/cm^2), a significant proportion of the recombination appears to occur on time scales less than the time resolution of this experiment (<100 ns). Note also that many previous literature reports of charge recombination have used excitation intensities >2mJ/cm^2, and may therefore be complicated by such nonlinear issues.[14−16] To avoid such nonlinear effects, all of our experiments were conducted using excitation powers corresponding to one photoinduced dye cation per TiO_2 particle, as we have employed previously.

We now consider the dependence of the charge recombination kinetics under externally applied electrical bias. The dye-sensitized TiO_2 film was included as the working electrode in a three-electrode electrochemical cell. An ethanol/0.1 M TBAT electrolyte was used (electrolyte A below); the potential of this electrolyte solution was kept constant by an Ag/AgCl reference electrode. Figure 2 shows absorption transients collected for potentials applied to the TiO_2 electrode ranging from +0.2 to −0.5 V vs Ag/AgCl. It is apparent that applied potentials of +0.1 and +0.2 V result in indistinguishable charge recombination kinetics. However, reduction in the applied voltage below 0 V causes a dramatic acceleration in these kinetics (10^4-fold for −0.5 V).

These studies were extended to more negative biases by ultrafast transient absorption measurements, as shown in Figure

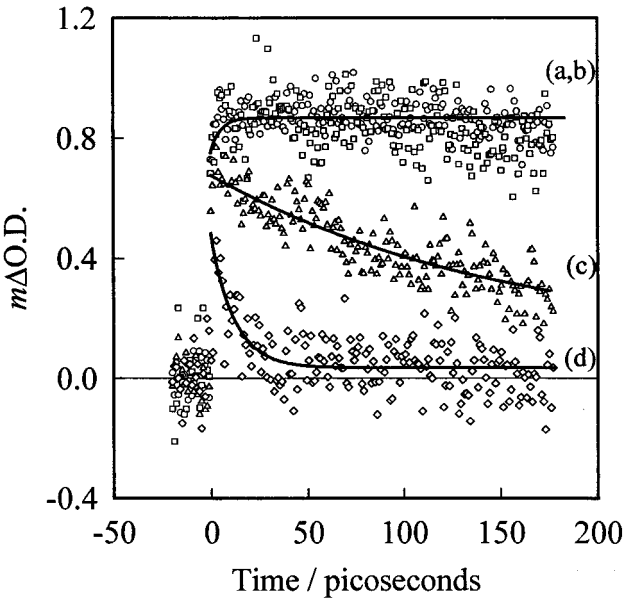

Figure 3. Transient absorption data collected on a 0−180 ps time scale for a $Ru(dcbpy)_2(NCS)_2$-sensitized TiO_2 electrode, as a function of applied biases between 0 and −800 mV vs Ag/AgCl. The data were collected in a three-electrode cell employing electrolyte A, as for Figure 2. Transient spectra were obtained between 680 and 780 nm, the transient kinetics obtained from these data are shown here for a probe wavelength of 760 nm. Data points are shown for (a) 0 (circle), (b) −400 (square), (c) −600 (triangle), and (d) −800 mV (diamond); solid lines are best fits to the data, employing a single-exponential component and a nondecaying background.

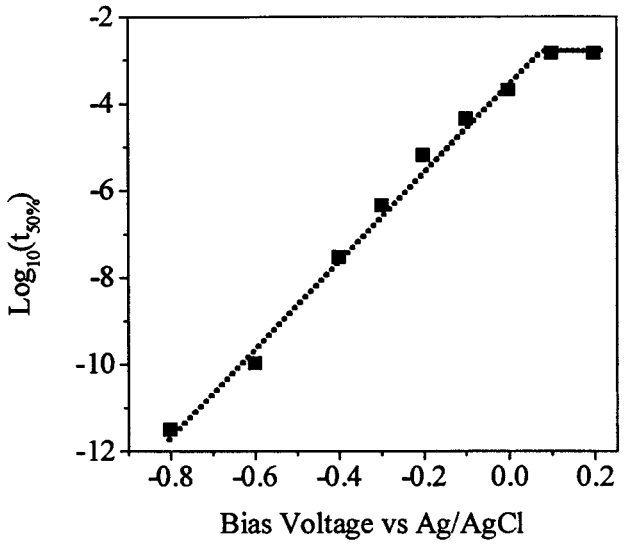

Figure 4. Plot of log $t_{50\%}$ versus applied potential to the dye-sensitized TiO_2 electrode, where $t_{50\%}$ was defined for each value of V as the time t at which the ratio (ΔOD (t, V)/ΔOD (20 ns, 0 V)) equalled 0.5. $t_{50\%}$ were determined from the data shown in Figures 2 and 3, employing an ethanol/0.1 M TBAT electrolyte (electrolyte A).

3. Data collected on this 0−180 ps time scale were independent of applied potentials up to −0.5 V. At −0.6 V, the transient signal is observed to decay with lifetime of 100 ± 30 ps, attributed to picosecond charge recombination induced by this applied bias. The amplitude of the initial transient signal and the transient spectrum at early times (∼10 ps), however, were unchanged by the application of this potential, indicating that the electron injection efficiency was invariant up to −0.6 V. A further acceleration of the decay rate to 3 ± 1 ps was observed by the application of −0.8 V. However, at this more negative potential, the initial amplitude of the signal is also reduced. This reduction in amplitude may result from a reduction in the injection yield at this potential.[36] A more complete consideration of the injection kinetics as a function of applied bias is given elsewhere.[11] We thus conclude that the recombination rate in this system can be varied from the millisecond to picosecond time scales simply by modulation of the potential applied to the TiO_2 electrode.

The temporal shape of the recombination kinetics shown in Figure 2 can be approximately fitted to a stretched exponential function (Δ OD $\propto \exp[-(t/\tau)^{\alpha}]$). A full kinetic analysis of these data is presented elsewhere. For the purposes of this paper, consideration of the time taken for 50% of the initially formed dye cations to decay ($t_{50\%}$) provides a reasonable quantification of the recombination time.[23] Figure 4 shows a plot of log $t_{50\%}$ versus applied bias determined from the data shown in Figures 2 and 3. It is evident that the graph exhibits a plateau region at positive biases (+0.1 and +0.2V), and a linear dependence of log $t_{50\%}$ versus V for more negative potentials (one decade change of rate every 100 mV). The acceleration in charge recombination under negative bias has been reported previously and attributed to the increased occupation of conduction band/trap states of the TiO_2 film under negative bias.[23]

The data shown in Figures 2 and 3 were collected with an ethanolic electrolyte. Comparable data were collected for a range of different redox inactive electrolytes, including protic and aprotic solvents (ethanol and acetonitrile, respectively). For the aprotic solvent (acetonitrile) the effects of water content, Li^+ content, and the addition of an adsorbate 4-*tert*-butylpyridine were addressed. Li^+ and 4-*tert*-butylpyridine were selected because they are widely used additives in the electrolyte of dye-sensitized photoelectrochemical devices, and because they have been found to improve device performance.[2] Addition of 4-*tert*-butylpyridine to the electrolyte solution has been found to increase the open circuit voltage of the device, which has been suggested to arise from the suppression of the dark current.[2]

We find that the transient kinetics observed under externally applied bias are strongly dependent upon electrolyte composition. Example data are shown in Figure 5, with the potential applied to the TiO_2 electrode held at −0.4 V versus the Ag/AgCl reference electrode. Data are shown for three electrolytes: (A) ethanol/0.1 M TBAT (as used for Figures 2 and 3), (B) acetonitrile/TBAP/0.1 M $LiClO_4$, and (C) acetonitrile/TBAP/0.1 M $LiClO_4$/0.5 M 4-*tert*-butylpyridine. At this fixed potential, the data show a remarkable difference in the rate of charge recombination as a function of electrolyte composition ($t_{50\%}$ varying by 10^6).

Transient data were collected, as a function of applied bias, for all three of the electrolyte compositions employed in Figure 5. Figure 6 shows a plot of log [$t_{50\%}$] versus applied potential V determined from these data. In each of the three cases log [$t_{50\%}$] shows a linear dependence upon applied potential V at negative potentials, and a plateau region in which $t_{50\%}$ is independent of applied potential for more positive potentials. The principle effect of the electrolyte/solvent composition upon the kinetics of charge recombination is to induce a lateral shift in the onset of bias dependence. For each electrolyte system we can therefore define an onset potential V_{kin} corresponding to the potential at which the transient kinetics become bias dependent. This corresponds to 0, −200, and −500 ± 50 mV for electrolytes A, B, and C, respectively.

The strong dependence of the charge recombination kinetics upon electrolyte composition appears not to be primarily associated with differences in the solvation of the dye itself,

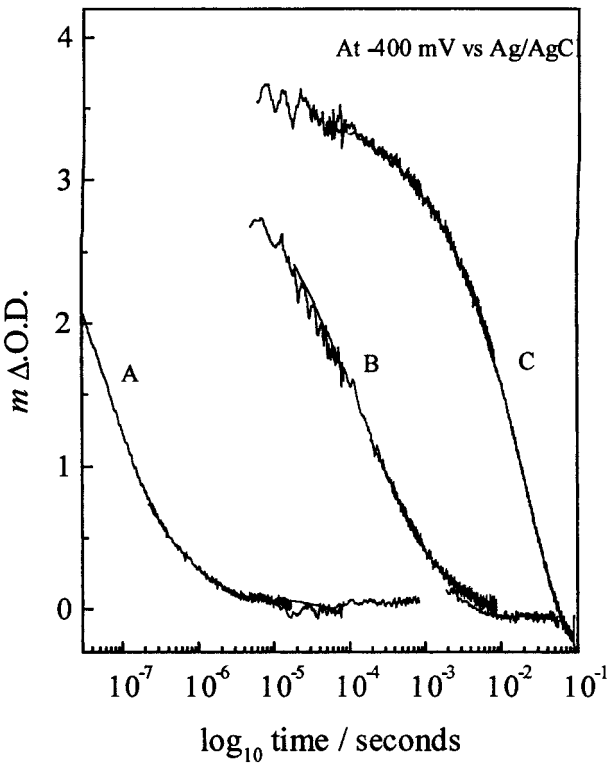

Figure 5. Transient absorption data following the decay of the cation state of $Ru(dcbpy)_2(NCS)_2$ adsorbed on TiO_2 nanocrystalline electrode. Data shown are held at a constant potential of −400 mV versus Ag/AgCl. Data shown were ascertained for three different solvent/electrolyte environments; (A) ethanol and 0.1 M TBAT; (B) dry acetonitrile with 0.1 M TBAP and 0.1 M lithium perchlorate; and (C) dry acetonitrile with 0.1 M TBAP, 0.1 M lithium perchlorate, and 0.5 M 4-*tert*-butylpyridine.

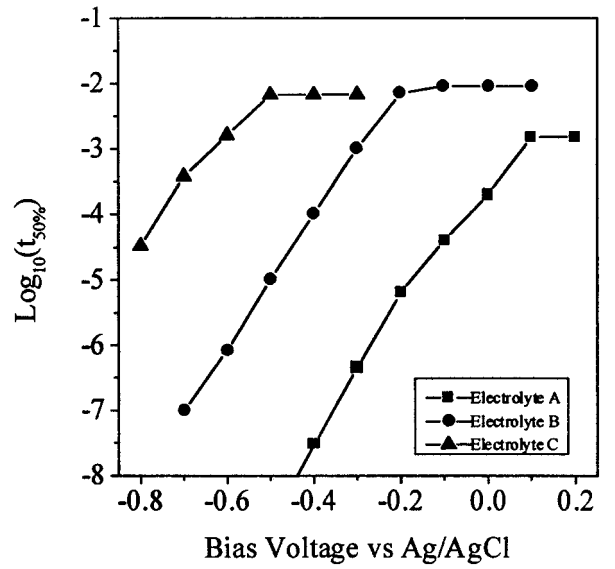

Figure 6. Plot of log $t_{50\%}$ versus applied potential to the dye-sensitized TiO_2 electrode for different electrolyte/solvent conditions. Electrolytes A (■), B (●), and C (▲) as for Figure 5.

nor with differences in the yield of electron injection. The electron injection yield (observed under more positive bias conditions in which charge recombination on time scales faster than the experimental time resolution can be neglected), was independent of electrolyte composition (to within experimental error of ±20%).[39] Moreover, in the absence of any applied electrical circuit, or under positive applied potentials ($V > V_{kin}$)

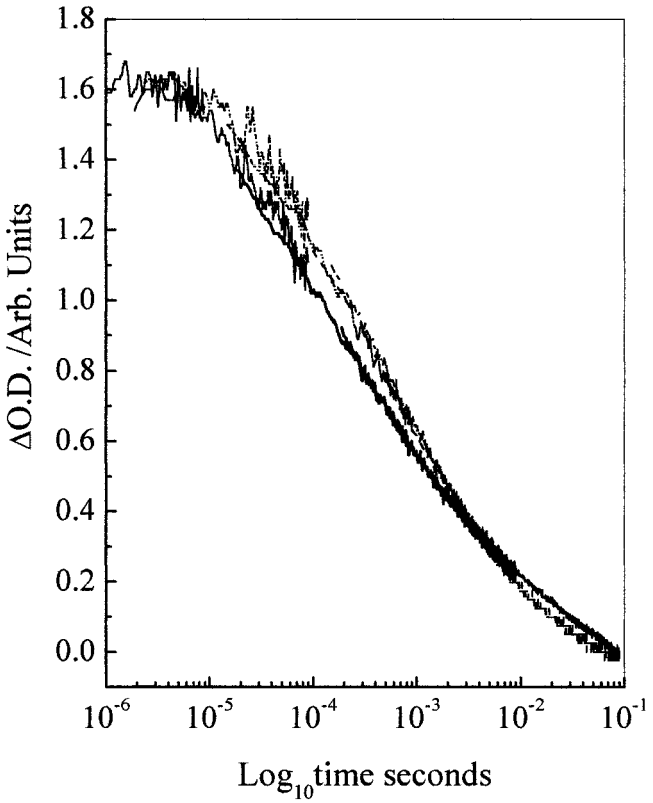

Figure 7. Transient absorption decay of the cation state of $Ru(dcbpy)_2(NCS)_2$ adsorbed on a nanocrystalline TiO_2 electrode. Data shown are for two different conditions ascertained without any electrical connection. (—) Electrolyte A (as in Figure 5); (- - -) no solvent (dried in air).

the charge recombination kinetics were only weakly dependent upon electrolyte composition. This is illustrated, for example, in Figure 7, which shows the charge recombination kinetics observed without any external electrical circuit for films dried in air and immersed in electrolyte B. The kinetics are almost indistinguishable, indicating that solvation of the dye by this electrolyte does not influence the kinetics. A similar conclusion can be drawn from the observation that the "plateau" regions observed in Figure 6 all exhibit rather similar $t_{50\%}$ values, independent of electrolyte composition.

The addition of either lithium ions or water to anhydrous acetonitrile electrolytes resulted in a positive shift in V_{kin} consistent with previous observations of the influence of $[Li^+]$ and pH on the flatband potential of such films.[26] A more quantitative analysis of the effect of different electrolyte compositions was provided by comparison with spectroelectrochemical studies. The application of negative potentials to nanocrystalline TiO_2 films results in a broad absorption increase attributed to optical absorption of electrons occupying conduction band/intraband states of the film. Monitoring of this absorption increase as a function of applied potential is therefore a crude measure of the occupancy of these states, and therefore the electronic density of states of the film.[21] Following this procedure, spectroelectrochemical data were collected (Figure 8) using the same electrolyte solutions A, B, and C.[41] Figure 8a shows the absorption spectra as a function of applied bias for electrolyte B; Figure 8b follows the absorption increase at a single wavelength as a function of applied bias for all three electrolytes. It is apparent that the different electrolytes result in shifts in the potential dependence of the absorption increase. Following published extinction coefficients for this absorption increase (1500−3000 M cm^{-1} at 800 nm[31]), an increase in electron occupancy of one electron/nanoparticle should give rise

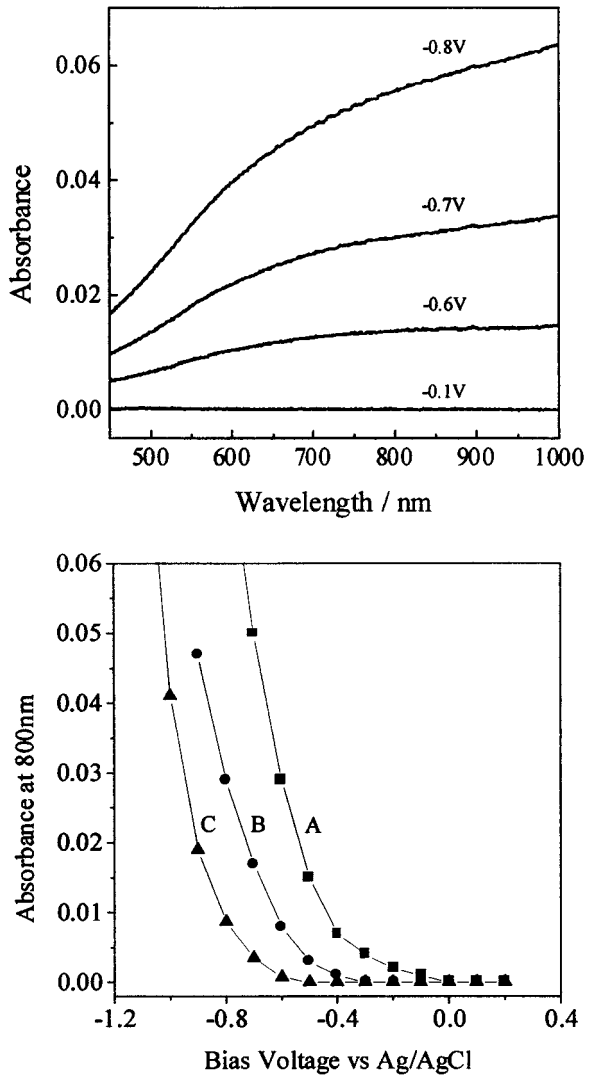

Figure 8. Spectroelectrochemical data showing (a) the absorption spectrum of a TiO_2 electrode in electrolyte B. Measured at −0.1, −0.6, −0.7, and −0.8 V vs Ag/AgCl reference electrode. (b) Optical absorbance at 800 nm of a TiO_2 electrode measured as a function of applied potential for three electrolytes, as in Figure 5.

to an absorption increase of ∼0.0005. From Figure 8, we thus conclude that the potential at which this increase in absorption is observed (V_{abs}) corresponds to 0, −300, and −500 ± 50 mV for electrolytes A, B, and C, respectively.

Figure 9 considers the correlation between V_{kin}, the onset of the bias dependence of the charge recombination kinetics, with V_{abs}, the onset of the steady-state absorption increase monitored spectroelectrochemically. It is apparent that there is a direct correlation between these two parameters. V_{kin} and V_{abs} were collected for a range of different electrolytes in addition to those considered in Figures 5−8; these data are also included in Figure 9 as indicated. The data points exhibit a clear linear dependence between V_{kin}, determined from transient charge recombination kinetics, and V_{abs} determined from spectroelectrochemical measurements of TiO_2 electron occupancy. The data fit well to a straight line with unity gradient, going through the origin. This straight line fit clearly demonstrates that the kinetics of charge recombination are strongly dependent upon the occupancy of conduction band/intraband states of the TiO_2 electrode. A rapid acceleration of the recombination kinetics is observed when the applied bias results in an increase in the occupancy of states by ≥1 ± 0.5 electrons/nanoparticle.

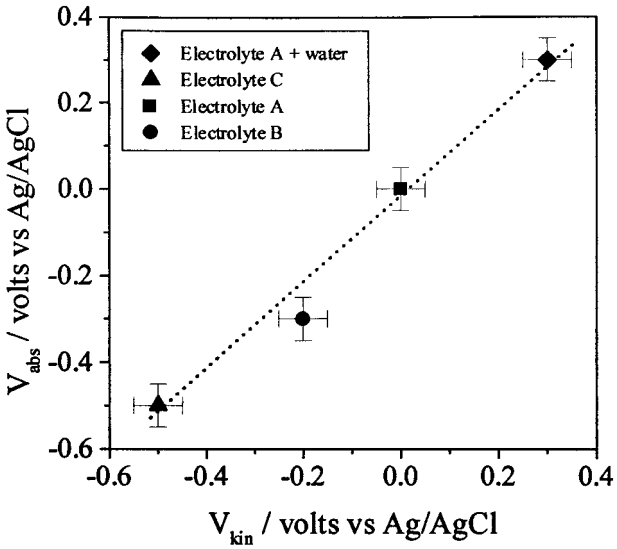

Figure 9. The linear correlation between V_{kin}, the onset of bias dependence of charge recombination kinetics, and V_{abs}, the onset of steady-state absorption increase monitored spectroelectrochemically. Data are shown for different solvent/electrolyte compositions. Data plotted exhibit a linear relationship with a gradient of 1. Data are shown for four different electrolytes: (■) electrolyte A, (●) electrolyte B, (▲) electrolyte C, and (◆) electrolyte A exposed to air (undried).

Discussion

In this paper we have considered the influence of a range of parameters upon the kinetics of charge recombination following photoinduced electron injection from an adsorbed sensitizer dye into the conduction band of nanocrystalline TiO_2 electrodes. We have demonstrated that these recombination kinetics are dependent upon laser excitation power, applied bias, and electrolyte composition. For all three cases, the dependence is strong (up to 10^8-fold). Such large variations in recombination rate may have a significant impact upon the performance of photoelectrochemical solar cells. As we discuss below, the large variations observed for all three parameters can be understood in terms of the electronic occupancy of conduction band/trap states of the TiO_2 film.

TiO_2 Electronic Density of States. Several groups have reported the existence of a high density of sub-bandgap or "trap" states lying below the conduction band edge of nanocrystalline titanium dioxide.[1,26−28] These states have been assigned to Ti^{3+} states.[29] The high density of these states has been associated, at least in part, with the high surface area/volume ratio of these films.[1,2] Several studies, including our own,[30] have indicated that these sub-bandgap states result in an exponential tail to the conduction band density of states. It should be noted that in this case the distinction between "conduction band" and "trap" states, and therefore of a "conduction band edge" is poorly defined. In this paper we refer only to the overall density of states of conduction band and trap states taken together.

It has been suggested that sub-bandgap states are active in mediating electron-transfer processes in these films.[42] We have also suggested that the occupancy of these states will have an influence upon the charge recombination kinetics.[23] Specifically, we suggested that dye cation states may recombine not only with electrons injected into the TiO_2 by photoinduced electron transfer from the excited dye, but also with electrons occupying TiO_2 conduction band/trap states due to the application of an external electrical bias (contrary to previous suggestions[49]). The data we present here provide strong evidence to support this conclusion.

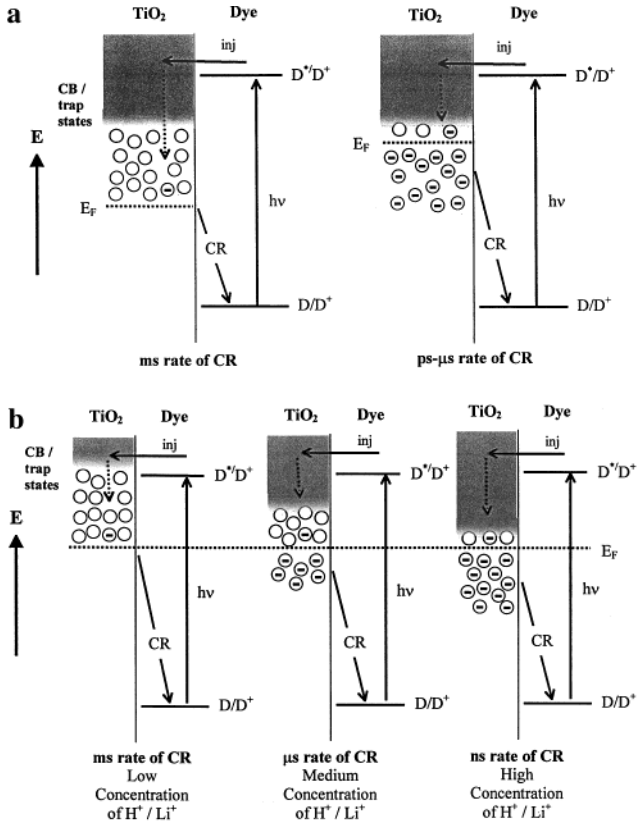

Figure 10. Schematic representation of electron-transfer processes in dye-sensitized TiO_2 film showing the variation in occupancy of conduction band/trap states as a function of (a) externally applied bias and (b) variation of solvent/electrolyte composition. Unoccupied trap states are indicated by (circle) and occupied states by (dash-circle). (a) The application of a negative potential results in an increase in the occupation of electrons in conduction/trap states of the titanium dioxide film. This increase in electron occupancy results in a rapid acceleration of the rate of charge recombination (CR) by up to 10^8. (b) The variation of the electrolyte composition results in a shift of the conduction band/trap state energetics. At a fixed bias this shift has a strong influence on the occupancy of the conduction/trap states. This results in a modulation of the rate of the charge recombination kinetics by up to 10^6. For simplicity, this figure neglects any possible influence of the electrolyte composition and applied bias on the dye redox potentials;[46] such dependencies are, however, not the primary focus of this paper.

Charge Recombination Kinetics. The application of an external bias to a nanocrystalline TiO_2 film modulates the Fermi level of this film.[43] If the Fermi level approaches or exceeds the potential of the conduction band/trap states, then the occupancy of these states will increase, as illustrated in Figure 10a. This will result in an increase in the rate of charge recombination.

Following this description, it is possible to rationalize the bias dependence of the charge recombination kinetics shown in Figures 2 and 3. The logarithmic dependence of the median recombination time, $t_{50\%}$, upon applied bias is consistent with simple Boltzmann considerations of electron occupancy[23] and/or with an exponentially increasing density of states. The bias independence at positive applied potentials results from the electron occupancy induced by the applied potential falling to less than one per nanoparticle. Under such conditions, the occupancy induced by the applied bias is less than that induced by the laser excitation (approximately one photoinjected electron per nanoparticle) and the charge recombination will therefore be dominated by electrons injected by the laser excitation.

This description is further supported by the dependence of the recombination kinetics upon excitation intensity in the absence of externally applied bias. At low excitation intensities (one injected electron per nanoparticle), the kinetics are independent of excitation power. However, as the excitation power is increased, the occupancy of conduction band/trap states induced by the laser excitation increases to $\gg 1$ per nanoparticle, and therefore there is an acceleration in the initial rate of charge recombination. Note also that the observed power independence for powers less than one injected electron per nanoparticle suggest that under the conditions of no externally applied bias and low excitation power the kinetics are limited by processes occurring within a single nanoparticle. In other words, the recombination is geminate, and under these low occupancy conditions an electron injected into one nanoparticle of the film will recombine with a dye cation on the same particle.

This model is moreover in agreement with our studies as a function of electrolyte composition. It is well established that variations in electrolyte composition result in large shifts in the conduction band density of states.[32] These shifts have been attributed to the intercalation/surface binding of small cationic "potential determining" ions including protons and Li^+. At a fixed applied potential, these shifts in the density of states will result in large variations in the occupancy of this density of states (Figure 10b). These variations in electron occupancy should have a large effect upon kinetics of charge recombination, as illustrated in Figure 5.

Quantitative support for this model comes from comparison of the bias dependence of electron occupation monitored spectroelectrochemically and the bias dependence of the recombination kinetics. Figure 9 illustrates that the applied potential at which the occupancy of the conduction band/trap states reaches $\sim$ one electron/nanoparticle, measured spectroelectrochemically, is the same, within error, as that at which the transient kinetics start to show an acceleration in the recombination rate. This direct correlation is the same for a variety of electrolytes, including protic and aprotic solvents, and the addition of Li^+ ions or 4-*tert*-butylpyridine. This observation has important implications for the optimization of electrolyte composition in dye-sensitized photovoltaic devices, as will be discussed further below.

It should be emphasized that the dependence of charge recombination kinetics upon electrolyte composition results from the influence of the electrolyte upon the TiO_2 and is not associated, to a first approximation, with differences in the solvation of the sensitizer dye. This conclusion is strongly supported by the data shown in Figure 7 collected for a TiO_2 film dried in air and immersed in anhydrous electrolyte (electrolyte B), but in the absence of any electrical connection to the TiO_2. The charge recombination kinetics in the absence of electrical connection are independent of electrolyte composition for anhydrous solvents (see, for example, Figure 7), indicating that differences in solvation have a negligible effect upon the recombination. The observation that the electrolyte dependence of the recombination kinetics is only observed with electrical connection to the TiO_2 can again be understood in terms of electron occupancy of conduction and/trap states of the TiO_2. In all cases the electrolytes employed were redox inactive. Therefore, in the absence of electrical connection to the TiO_2, variations in electrolyte composition are unable to modify the electron occupancy of the TiO_2 density of states, and the recombination kinetics are independent of electrolyte composition.

We further note that the strong dependence of the recombination kinetics upon applied bias and electrolyte composition is not correlated with variations in the yield of electron injection.[40]

Figures 2 and 3 demonstrate that for electrolyte A, the electron injection yield is independent of applied bias, at least for applied voltages ≥ -0.6 V. We present elsewhere data demonstrating a similar bias independence of the injection yield for studies employing electrolyte B. However, we note that, particularly for the acetonitrile electrolytes (B and C), prolonged application of more negative potentials resulted in an irreversible (or very slowly reversible) loss of injection yield. This observation is consistent with recent observations by Hupp and co-workers[55] and is tentatively assigned to desorption/degradation of the sensitizer dye. However, we emphasize that in the studies reported here such extreme conditions were avoided, and changes in the kinetics induced by the applied bias were fully reversible.

Mechanism of Charge Recombination. Charge recombination associated with dye-sensitized semiconductor films has previously been modeled in terms of Marcus electron transfer theory, involving consideration of the electronic coupling and reorganizational/free energy changes associated with the interfacial electron-transfer event.[44,45] The strong dependencies we observe here as a function of applied bias and electrolyte composition cannot be explained by such analyses. For example, the application of a more negative potential and a negative shift of the trap state/conduction band energetics would both be expected to increase the average free energy change associated with charge recombination. However, we observe that whereas the former results in an acceleration of the charge recombination kinetics, the latter results in a retardation of these kinetics (as illustrated in Figure 10). These opposing observations are clearly inconsistent with a simple Marcus analysis.

As detailed above, we suggest instead that these observations can be readily explained by the kinetics being strongly controlled by the occupancy of conduction band/trap states of the TiO_2. The extreme sensitivity of the recombination kinetics to applied bias is particularly remarkable. A simple second-order kinetic analysis would suggest that the recombination rate should be proportional to the number of conduction band/trap electrons/nanoparticle. However, Figure 4 illustrates that the application of a negative potential to the TiO_2 electrode can result in an increase in the recombination rate by up to 10^8. Because the slowest kinetics correspond to one electron/nanoparticle (the number injected by the laser pulse), such a simple second-order analysis would imply an electron density of $\sim 10^8$ electrons per nanoparticle. This is clearly implausible. It thus appears that the charge recombination kinetics exhibit a highly nonlinear dependence upon electron occupancy.

Our conclusion that the recombination kinetics exhibit a nonlinear dependence upon electron occupancy is inconsistent with simple second-order models for this reaction. However, such nonlinear dependencies on electron occupancy have been widely reported and discussed for random walk models of electron transport between trap sites distributed in energy and/or trap separation.[38] Indeed such a model, based upon continuous time random walk with an exponential distribution of trap depths, was recently shown to be in good agreement with the bias dependence of recombination kinetics reported here.[37] This model implies that the recombination kinetics are primarily controlled by the trapping/detrapping dynamics of electron transport within the TiO_2 nanoparticles, in good agreement with the experimental observation we report here and elsewhere.[7]

Electron transport models based on electron hopping between trap sites are consistent with the high density of trap states widely reported for nanocrystalline TiO_2 films.[1] More quantitative consideration of such models will, however, require careful consideration of the electronic conduction band/trap density of states. Such studies are complicated by the possible dependence of this density of states upon applied bias ("fermi level pinning"). Ambiguities associated with the spectroelectrochemical data preclude such analyses based on these data alone; alternative experiments to address these issues are currently in progress.

Although our observations indicate that the primary issue influencing the recombination kinetics is electron occupancy on TiO_2 conduction band/trap states, this does not imply that issues such as electronic coupling and the reorganizational/free energy do not have some influence these kinetics. We report elsewhere[7] upon our comparison of the charge recombination observed for three different sensitizer dyes, $Ru(dcbpy)_2(NCS)_2$ and zinc/free base tetracarboxyphenyl porphyrins (ZnTCPP/H_2-TCPP). In particular, we note that H_2TCPP exhibited a $\sim$5−8-fold slower charge recombination than ZnTCPP. This difference can be rationalized in terms of a Marcus analysis of the rate of interfacial electron transfer as being due to the 0.4 V difference in midpoint potential of these dyes in solution, although such redox arguments are complicated by possible shifts in the dye redox potentials induced by adsorption.[46] Such dependencies of the recombination rate upon free energy gap have also been reported eleswhere. However, it is important to note that this difference in rate is much smaller than the dependence upon electron occupancy which is the primary focus of this paper.

Comparison with Other Studies. Previous studies of charge recombination dynamics for dye-sensitized TiO_2 have differed widely in the time constants reported. Studies of charge recombination in dye-sensitized nanocrystalline TiO_2 films exhibited time constants ranging from $\sim$tens of picoseconds to approximately 1 ms.[12−21,47,48] Several studies considered the influence of applied bias voltage, but again with widely differing results. For example, whereas O'Regan et al. reported a 10^3-fold acceleration in recombination rate as a function of applied negative bias, Kamat and co-workers reported that the recombination kinetics were independent of applied bias.[47,48]

We have demonstrated here that the kinetics of charge recombination are strongly dependent upon the occupancy of conduction band/trap states of the TiO_2 film. We can rationalize much of the variation in experimental observations in the literature on the basis of this conclusion. Most literature studies have employed higher laser powers than we have used here. As we demonstrate in Figure 1, this results in a rapid acceleration of the charge recombination processes. Moreover, because of the high electron occupancy induced by the laser pulse, the effects of modulation of the electron density by applied electrical bias are likely to be less pronounced. In addition, the influence of electrolyte composition upon electron occupancy and thereby charge recombination has not previously been considered. As we demonstrate in Figure 5, this effect can be very large. However, under no externally applied bias and moderate applied bias conditions where a "plateau region" is observed there is only a weak dependence of electrolyte composition upon the charge recombination kinetics (see Figures 6 and 7). This observation is in agreement with that of Hupp and co-workers, who reported analogous studies of charge recombination kinetics which were observed to be independent of the pH of the electrolyte under open circuit conditions.[19]

Steady state and frequency domain photovoltage and photocurrent studies have been widely used to study the electron transfer and transport properties of dye-sensitized photovoltaic devices. Such studies have, however, not addressed specifically

the importance of charge recombination between injected electrons and dye cation, or have assumed this reaction to be linearly dependent upon electron concentration.[49−52] Our observation that the recombination kinetics exhibit a nonlinear dependence upon electron occupancy, accelerating at negative potentials to time scales likely to be fast relative to the iodide rereduction of the dye cation, calls into question this assumption. We further note that this dependence upon electron occupancy results in the recombination kinetics being very sensitive to electrolyte composition, a consideration neglected in a recent quantitative comparison of frequency and time domain studies of charge recombination.[53]

Note that although we have demonstrated that electron occupancy of conduction band/trap states is a key parameter controlling the charge recombination kinetics, it is unlikely to be the only parameter. For example, it is apparent that there is a significant variation in the $t_{50\%}$ for charge recombination in "plateau" potential independent regions shown in Figure 6. Because all of these data should correspond to data collected with negligible occupancy prior to the optical excitation, this variation cannot be explained by variations in occupancy between the different conditions. This variation may result, at least in part, from variations in the water content of these electrolytes. However, it is important to note that this difference in rate, although reproducible, is again much smaller than the dependence upon electron occupancy which is the primary focus of this paper.

Relevance to Photoelectrochemical Solar Cells. In a functioning device, the charge recombination we have considered will result in a loss of photocurrent efficiency if its rate exceeds the rereduction of the dye cation by the iodide electrolyte. The results we have presented here were not obtained from a complete photoelectrochemical solar cell. In particular, they were obtained with a redox inactive electrolyte. We also note that the kinetics of dye cation rereduction by iodide ions are also dependent upon the electrolyte compostion.[25] Given the clear dependence of the recombination kinetics upon electrolyte composition, a rigorous comparison between these data and a complete cell with redox active electrolyte is not possible. Nevertheless, as we have indicated previously[23] the rapid acceleration in this recombination at negative applied bias may result in this recombination becoming an important loss mechanism as the cell output voltage is increased. As such this recombination would limit the open circuit voltage of the cell.

Several groups have reported that the addition of Li^+ and 4-*tert*-butylpyridine improve the current/voltage characteristics of the cell.[2] It is interesting to note that both Li^+ and 4-*tert*-butylpyridine are typically added in most recent studies of device performance. It is, however, apparent from Figure 9 that these additives have opposing effects upon the energetics of the conduction band/trap states and therefore on the kinetics of charge recombination (the addition of Li^+ shifts the states more positive, whereas 4-*tert*-butylpyridine shifts the states more negative). Although these additives may influence cell function in other ways not addressed here, it is apparent that at least in terms of their influence upon the charge recombination losses, the effects of these two additives are counterpoised.

Conclusion

We have shown that the kinetics of charge recombination between electrons injected into nanocrystalline TiO_2 films and adsorbed dye cations are strongly dependent upon the electron occupancy of trap/conduction band states of the film. This electron occupancy may be modulated by optically driven electron injection, or by the application of an external electrical circuit.

The observation of a dependence of recombination rate upon trap/conduction band electron occupancy is in itself not surprising. However, the magnitude of the observed dependency is remarkable. For example, variation of the external applied potential by only 600 mV results in a 10^7-fold acceleration of the recombination kinetics. Similarly, a 500 mV shift in the TiO_2 conduction band/trap density of states induced by variations in electrolyte composition results in a variation in recombination rate by up to 10^6. These large dependencies are inconsistent with second-order kinetic models of this reaction, but consistent with this reaction being controlled by electron transport between an energetic distribution of trap sites with the TiO_2 nanoparticles.[37] We further note that the large variations in recombination rate reported here have not been considered in previous models of the function of dye-sensitized nanocrystalline solar cells, and may play a role in limiting the performance of such devices.

Acknowledgment. We are very grateful to Dr. Pascal Comte and Dr. K. Nazeeruddin for the synthesis of the TiO_2 colloidal particles and the sensitizer dye, respectively. We would also like to thank Dr. Jenny Nelson for many helpful discussions concerning this study. We are also very grateful to Dr. Chris Barnett for his excellent technical support, and Libby Owen Ford and Asahi Glass Co. Ltd., for gifts of conducting glass. M.G. and J.E.M. acknowledge the support of the Swiss National Foundation. This work was supported by grants from EPSRC and BBSRC. Y.T. acknowledges the CVCP for the support of an ORS award.

References and Notes

(1) Hagfeldt, A.; Grätzel, M. *Chem. Rev*. **1995**, *95*, 49−68.
(2) Nazeerudin, M. K.; Kay, A.; Rodicio, I.; Humphrey-Baker, R.; Muller, E.; Liska, P.; Vlachopoulos, N.; Grätzel, M. *J. Am. Chem. Soc*. **1993**, *115*, 6382−6390.
(3) O'Regan, B.; Grätzel, M. *Nature* **1991**, *353*, 737−739.
(4) Tachibana, Y.; Moser, J. E.; Grätzel, M.; Klug, D. R.; Durrant, J. R. *J. Phys. Chem*. **1996**, *100*, 20056−20062.
(5) Cherepy, N. J.; Smestad, G. P.; Grätzel, M.; Zhang, J. Z. *J. Phys Chem. B*, **1997**, *101*, 9342−9351
(6) Durrant, J. R.; Tachibana, Y.; Mercer, I.; Moser, J. E.; Grätzel, M.; Klug, D. R. *Z. Phys. Chem.* **1999**, in press.
(7) Tachibana, Y.; Haque, S. A.; Mercer, I.; Klug, D. R.; Durrant, J. R. *J. Phys. Chem. B* **2000**, in press.
(8) Burfeindt, B.; Hannappel, T.; Storck, W.; Willig, F. *J. Phys. Chem*. **1996**, *100*, 16463−16465.
(9) Ellingson, R. J.; Asbury, J. B.; Ferrere, S.; Ghosh, H. N.; Sprague, J.; Lian, T.; Nozik, A. J. *J. Phys. Chem. B* **1998**, *102*, 6455−6458.
(10) Rehm, J. M.; McLendon, G. L.; Nagasawa, Y.; Yoshihara, K.; Moser, J.; Grätzel, M. *J. Phys. Chem*. **1996**, *100*, 9577.
(11) Tachibana, Y.; Haque, S. A.; Mercer, I.; Moser, J. E.; Klug, D. R.; Durrant, J. R. *J. Phys. Chem. B* **1999**, submitted for publication.
(12) Stipkala, J. M.; Castellano, F. N.; Heimer, T. A.; Kelly, C. A.; Livi, K. J. T.; Meyer, G. J. *Chem. Mater*. **1997**, *9*, 2341−2353.
(13) Hilgendorf, M.; Sundstrom, V. *J. Phys. Chem. B* **1998**, *102*, 10505−10514.
(14) Argazzi, R.; Bignozzi, C. A.; Heimer, T. A.; Castellano, F. N.; Meyer, G. J. *J. Phys. Chem. B* **1997**, *101*, 2591−2597.
(15) Argazzi, R.; Bignozzi, C. A.; Hasselmann, G. M.; Meyer, G. *J. Inorg. Chem.* **1998**, *37*, 4533−4537.
(16) Liu, D.; Fessenden, R. W.; Hug, G. L.; Kamat, P. V. *J. Phys. Chem. B* **1997**, *101*, 2583−2590.
(17) Argazzi, R.; Bignozzi, C. A.; Heimer, T. A.; Castellano, F. N.; Meyer, G. J. *J. Am. Chem. Soc*. **1995**, *117*, 11815−11816.
(18) Nazeeruddin, M. K.; Liska, P.; Moser, J. E.; Vlachopoulos, V.; Grätzel, M. *Helv. Chim. Acta* **1990**, *73*, 1788−1803.
(19) Yan, S.; Hupp, J. T. *J. Phys. Chem.* **1996**, *100*(17), 6867−6870.
(20) Kalyanasundaram, K.; Vlachopolous, N.; Krishnan, V.; Monnier, A.; Grätzel, M. *J. Phys. Chem.* **1996**, *100*, 2342−2347.

(21) Martini, I.; Hodak, J. H.; Hartland, G. V. *J. Phys. Chem. B* **1998**, *102*(3), 607−614.
(22) Alebbi, M.; Bignozzi, C. A.; Heimer, T. A.; Hasselmann, G. M.; Meyer, G. J.; *J. Phys. Chem. B* **1998**, *102*, 7577−7581.
(23) Haque, S. A.; Tachibana, Y.; Klug, D. R.; Durrant, J. R.; *J. Phys. Chem. B* **1998**, *102*(10), 1745−1749.
(24) Franco, G.; Gehring, J.; Peter, L. M.; Ponomarev, E. A.; Uhlendorf. I. *J. Phys. Chem. B* **1999**, *103*, 692−698.
(25) We also note that the regeneration of the oxidized dye by the iodide redox electrolyte has received limited attention to date. This dye regeneration reaction also exhibits a dependence upon electrolyte composition and externally applied bias. (Nasr, C.; Hotchandani, S.; Kamat, P. V. *J. Phys. Chem. B* **1998**, *102*, 4944−4951; and Pelet, S.; Moser, J. E.; Grätzel, M. *J. Phys. Chem. B*, in press.
(26) Redmond, G.; Fitzmaurice, D.; Grätzel, M. *J. Phys. Chem*. **1993**, *97*, 6951−6954.
(27) Rothenberger, G.; Moser, J. M.; Grätzel, M.; Serpone, N.; Sharma, D. K. *J. Am. Chem. Soc.* **1985**, *107*, 8054−8059.
(28) Kay, A.; Humphrey-Baker, R.; Grätzel, M. *J. Phys. Chem*. **1994**, *98*, 952−959.
(29) Howe, R. F.; Grätzel, M. *J. Phys. Chem*. **1985**, *89*, 4495−4499.
(30) Willis, R.; Haque, S. A.; Nelson, J.; Klug, D. R.; Durrant, J. R., to be submitted for publication.
(31) Rothenberger, G.; Fitzmaurice, D.; Grätzel, M. *J. Phys. Chem*. **1992**, *96*, 5983−5986.
(32) Redmond, G.; Fitzmaurice, D. *J. Phys. Chem*. **1993**, *97*, 1426−1430.
(33) Das, S.; Kamat, P. V. *J. Phys. Chem. B* **1998**, *102*(45), 8954−8957.
(34) In addition to the dye cation, induced absorption from electrons injected into the TiO_2 may also contribute to the transient signal at 800 nm. However, studies[35] of dye-sensitized TiO_2 in which the 800 nm dye cation absorption band is not present due to degradation of the NCS groups indicates that $Ru(dcbpy)_2(NCS)_2$ cation absorption accounts for ≥70% of the absorption at 800 nm. This conclusion is also in agreement with estimates of the extinction coefficients at 800 nm for the dye cation and electrons injected into the TiO_2,[4,31,54] and with comparisons to the difference spectra obtained for the $Ru(dcbpy)_2(NCS)_2$ cation state generated in solution.[4] Contributions to the transient data from dye-excited states can be neglected because of its relatively weak absorption at 800 nm and short excited-state lifetime (3−25 ns). We thus conclude that amplitude of the signal at 800 nm is primarily dominated by dye cation absorption.
(35) Moser, J. E.; Noukakis, D.; Bach, U.; Tachibana, Y.; Klug, D. R.; Durrant, J. R.; Humphrey-Baker, R.; Grätzel, M. *J. Phys. Chem. B* **1998**, *102*, 3649−3650.
(36) Note that the changes observed because of the application of −0.8 V were not fully reversible, indicating possible dye degradation or desorption induced at this potential.
(37) Nelson, J. *Phys. Rev. B* **1999**, *59*(20), 15374−15380.
(38) Blumen, A.; Kohler, G. H. In *Fractals in Natural Sciences*; Fleischmann, M., Tildeley, D. J., Ball, R. C., Eds.; Princeton University Press: 1989; pp 189−200.
(39) Ultrafast transient absorption studies of electron injection in $Ru(dcbpy)_2(NCS)_2$-sensitized TiO_2 films have demonstrated that the electron injection yield is near unity (>90%) for both electrolytes A and B.[6,11]
(40) No dependence of electrolyte composition upon the injection yield was observed for any of electrolytes employed in this study, determined both from the magnitude of the 800 nm signal observed on the nanosecond−millisecond time scales as reported here (to within ±20% experimental error) and from ultrafast studies of the electron injection kinetics and yield.
(41) Data shown were collected without adsorbed dye molecules; however, data collected with adsorbed dyes were indistinguishable, but this was limited to a smaller voltage range to avoid dye degradation.
(42) Schwartzburg, K.; Willig, F. *Appl. Phys. Lett*. **1991**, *58*, 2520−2522.
(43) It has been suggested that this modulation of Fermi level under applied bias is limited at low biases only to the film region adjacent to the conducting glass (ref 56). However, our own studies of this Fermi level distribution indicate that under our experimental conditions the Fermi level is distributed uniformly throughout the film. This issue will be addressed in detail elsewhere. Haque, S. A.; Klug, D. R.; Durrant, J. R., to be submitted for publication.
(44) Heimer, T. A.; Bignozzi, C. A.; Meyer, G. J. *J. Phys. Chem*. **1993**, *97*, 11987−11994.
(45) Moser, J. E.; Grätzel, M. *Chem. Phys.* **1993**, *176*, 493−500
(46) Zaban, A.; Ferrere, S.; Gregg, B. A. *J. Phys. Chem. B* **1998**, *102*, 452−460.
(47) O'Regan, B.; Moser, J.; Anderson, M.; Grätzel, M. *J. Phys. Chem.* **1990**, *94*, 8720−8726.
(48) Kamat, P. V.; Bedja, I.; Hotchandani, S.; Patterson, L. K. *J. Phys. Chem.* **1996**, *100*, 4900−4908.
(49) Dloczik, L.; Ileperuma, O.; Lauermann, I.; Peter, L. M.; Ponomarev, E. A.; Redmond, G.; Shaw, N. J.; Uhlendorf, I. *J. Phys. Chem. B* **1997**, *101*, 10281−10289.
(50) De Jongh, P. E.; Vanmaekelbergh, D. *J. Phys. Chem. B* **1997**, *101*, 2716−2722
(51) Schlichthorl, G.; Huang, S. Y.; Sprague, J.; Frank, A. J. *J. Phys. Chem. B* **1997**, *101*, 8141−8155.
(52) Schlichthorl, G.; Park, N. G.; Frank, A. J. *J. Phys. Chem. B* **1999**, *103*, 782−791.
(53) Franco, G.; Gehring, J.; Peter, L. M.; Ponomarev, E. A.; Uhlendorf, I. *J. Phys. Chem. B* **1999**, *103*, 692−698.
(54) Bach, U.; Tachibana, Y.; Moser J. E.; Haque, S. A.; Durrant, J. R.; Grätzel, M.; Klug, D. R. *J. Am. Chem. Soc*. **1999**, *121*, 7445−7446.
(55) Lemon, B. I.; Hupp, J. T. *J. Phys. Chem. B* **1999**, *103*, 3797−3799.
(56) Zaban, A.; Meier, A.; Gregg, B. A. *J. Phys. Chem. B.* **1997**, *101*, 7985−7990.